Identification of the damped harmonic oscillator frequency response function from base acceleration and interface force

C. Schedlinski [1], W. Jaenich [2]
[1] ICS Engineering GmbH,
Am Lachengraben 5, D-63303 Dreieich, Germany
e-mail: **info@ics-engineering.com**

[2] Gartenstraße 3, D-73466 Lauchheim, Germany

Abstract
In this paper an approach is presented to identify the frequency response function of a simple damped harmonic oscillator (one mass spring/damper system) under base excitation without the need for measuring the dynamic motion of the oscillating mass itself. The approach solely makes use of the measured base acceleration and the corresponding base force. The theoretical foundation of the procedure is outlined at first. Then, basic considerations are highlighted based on a Finite Element model of the damped harmonic oscillator and the relevant test bench parts. Finally results from real test data are presented to prove the applicability of the method.

1 Introduction

For vibration damping of, e.g., an optical system enabling chip makers to produce microchips, simple damped harmonic oscillators (DHO → one mass spring/damper systems) can be employed. Here, proper tuning of the resonance frequencies of the DHOs is mandatory in order to guarantee proper performance of the overall system.

Hence, a test bench needs to be developed to determine the frequency response function (FRF) of the DHO from which the resonance frequency (and damping) can be identified subsequently. Since accessibility of the oscillating mass of the DHO can be limited and an application of acceleration sensors can be rather problematic (e.g., due to clean room conditions), an approach was developed by **ICS** to obtain the dynamic motion of the oscillating mass from base excitation data while the dynamic motion is indirectly identified from base acceleration and base (interface) force data.

In this paper the theoretical foundation of the procedure is outlined at first. Then, basic considerations are highlighted based on a Finite Element model of the DHO and the relevant test bench parts. Finally results from real test data are presented to prove the applicability of the method.

2 Theoretical background

Basis for the approach is the two mass/two degrees of freedom DHO outlined in Figure 1. Here, “1” refers to the base and “2” to the oscillating mass.

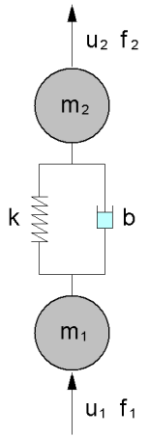

Figure 1: Damped harmonic oscillator (DHO)

Now, for the DHO the equation of motion with structural damping according to (1) can be employed in the frequency domain as:

$$\left[-\omega^2\begin{bmatrix} m_1 & 0 \\ 0 & m_2 \end{bmatrix} + jb\begin{bmatrix} k & -k \\ -k & k \end{bmatrix} + \begin{bmatrix} k & -k \\ -k & k \end{bmatrix}\right]\begin{bmatrix} u_1 \\ u_2 \end{bmatrix} = \begin{bmatrix} f_1 \\ f_2 \end{bmatrix} \tag{1}$$

Equation (1) yields two equations (2a) and (2b):

$$-\omega^2 m_1 u_1 + jbku_1 - jbku_2 + ku_1 - ku_2 = f_1 \tag{2a}$$

$$-\omega^2 m_2 u_2 - jbku_1 + jbku_2 - ku_1 + ku_2 = f_2 \tag{2b}$$

Simply adding (2a) and (2b) gives us equation (3):

$$-\omega^2 m_1 u_1 - \omega^2 m_2 u_2 = f_1 + f_2 \tag{3}$$

For pure base excitation f_2 will be zero. Considering as well accelerations instead of displacements (i.e. $a_\mathrm{i} = -\omega^2 u_\mathrm{i}$) equation (3) becomes:

$$m_1 a_1 + m_2 a_2 = f_1 \tag{4}$$

Solving for the desired motion of the oscillating mass a_2 finally gives:

$$a_2 = \frac{f_1}{m_2} - \frac{m_1}{m_2} a_1 \tag{5}$$

From equation (5) it can be seen that the motion of the oscillating mass a_2 can easily be computed when base acceleration and force as well as the masses m_1 and m_2 are known.

2.1 Test bench

2.1.1 Design concept

The basic concept of the test bench is to apply base excitation via an electrodynamic shaker system in vertical direction. Next to an acceleration measurement in vertical direction the vertical interface force must be measured as well. To accomplish this, a special force measurement device (FMD) was developed at **ICS**.

In Figure 2 the concept with FMD is shown. The individual parts are as follows:

1. Shaker interface plate
2. FMD base plate
3. Acceleration sensor (uniaxial pilot sensor)
4. Force sensor (uniaxial, three under 0°/120°/240°, equal radial positions)
5. FMD upper plate (interface to DHO)
6. DHO base mass, shown here: Fumo (stiff functional model)

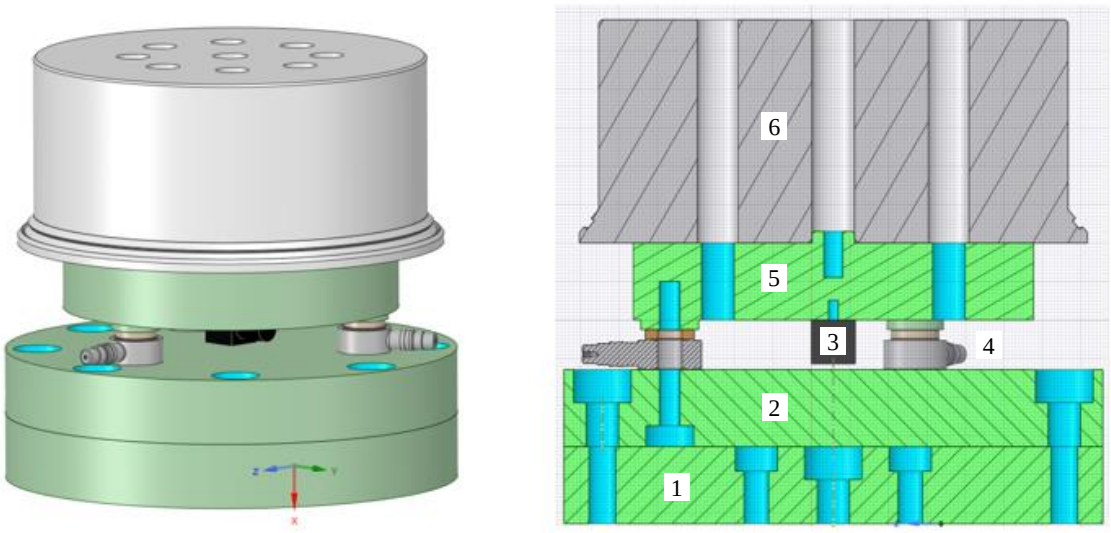

Figure 2: Survey of test bench (w/o oscillating mass)

The base acceleration is measured straight forward with a standard uniaxial acceleration sensor (3 in Figure 2) with adequate sensitivity. The base force is derived by averaging the three measured forces from the individual force sensors (4 in Figure 2). It should me mentioned that special care must be taken with respect to selection of the force sensors. Here, a dedicated set was assembled with all sensors grinded by the manufacturer to equal height. Also, the FMD plates (2 and 5 in Figure 2) must be grinded or adequately milled at the force sensor assembly positions. This is necessary to avoid improper bracing of the sensors later during assembly of the FMD.

The base mass m_1 according to Equation (5) comprises of the complete seismic mass above the measurement plane of the force sensors. In detail, of the seismic mass of the force sensors (mass above force measurement plane), acceleration sensor mass including seismic cable mass, FMD upper plate, DHO base mass, and the bolts required for assembly. This mass and the oscillating mass m_2 can easily be derived with sufficient accuracy from weighing (masses of the spring/damper system are equally distributed to base and oscillating mass).

Finally, a shaker with sufficient suspension stiffness must be utilized in order to avoid parasitic cross talk of the system under test. Optionally damping mats may be used in addition between shaker interface plate (1 in Figure 2) and the shaker itself to mitigate effects of eventual cross talk.

2.1.2 Analytical study

The DHO under investigation is available in two configurations: first with a stiff base (“Fumo”) and second with a flexible base (“Series”). Now, the fundamental assumption for Equation (5) is that both masses are ideally stiff. Obviously, this will not necessarily be the case in reality, especially for the Series DHO. Therefore, an analytical study based on Finite Element (FE) calculations was conducted to pinpoint the weak spots in the concept. Figure 3 shows the FE model used for the investigations. Red is the Series base, green the oscillating mass (m_2), light blue the FMD upper plate, and dark blue the FMD base plate

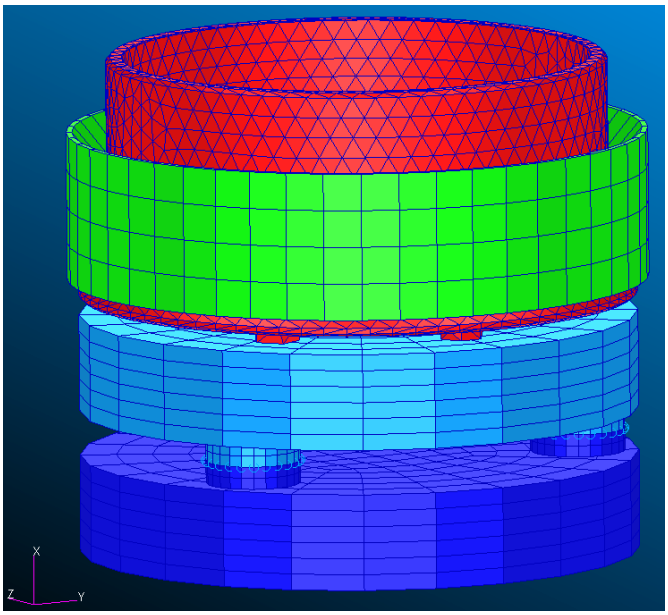

Figure 3: FE-Model of test bench

Figures 4 through 6 show results for different configurations of the FE model. In Figure 4 all parts are elastic and the ideal FRF is shown next to the FRF computed from Equation (5). It can be noticed, that a significant systematic error is introduced by the elasticity of the parts.

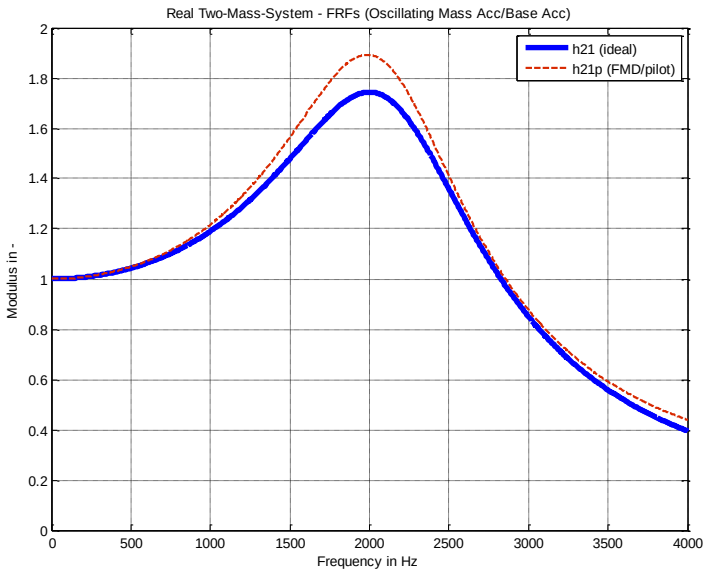

Figure 4: Ideal FRF (h21) vs. FRF (h21p) according to Equation (5) – initial FE model

To assess the individual influences of FMD and Series DHO base, two variants were analyzed in addition. In Figure 5 only the FMD was stiffened in order to remove the effects of the FMD's elasticity, in Figure 6 only the Series DHO base was stiffened. It can be seen that the elasticity of the Series DHO base has the driving impact on the accuracy of the results.

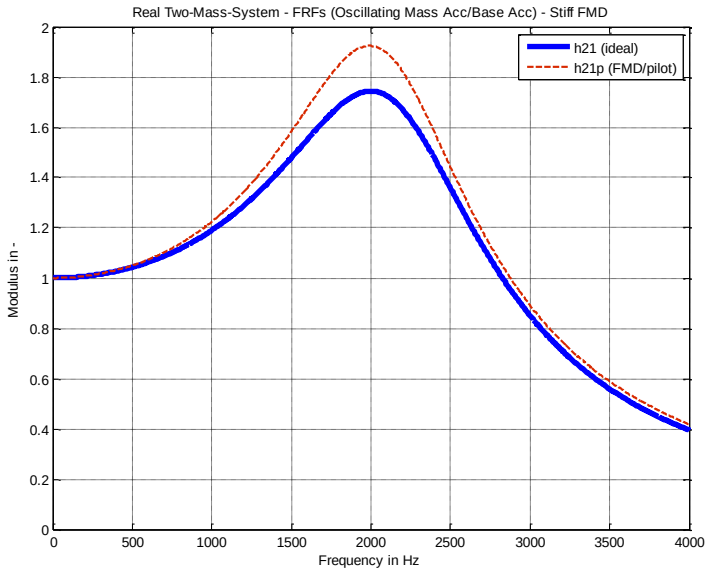

Figure 5: Ideal FRF (h21) vs. FRF (h21p) according to Equation (5) – FMD stiffened

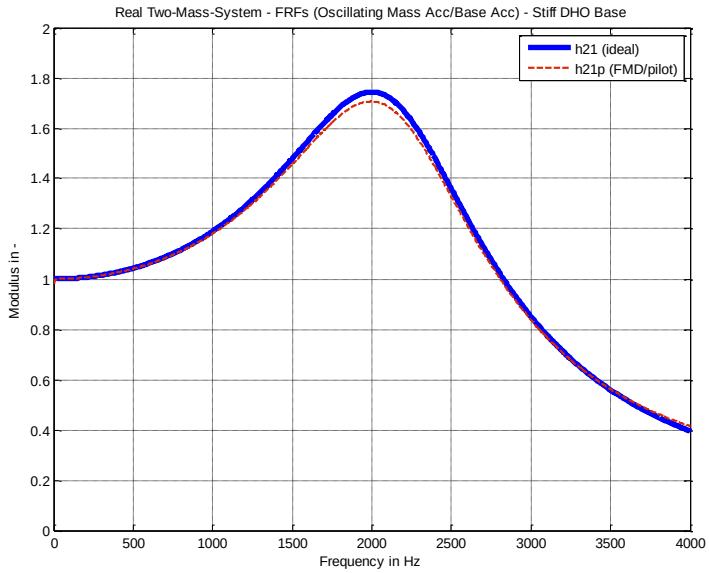

Figure 6: Ideal FRF (h21) vs. FRF (h21p) according to Equation (5) – Series DHO base stiffened

Since the elasticity of the Series DHO base will, of course, be present in reality, a modification of the mounting situation of the DHO base to the FMD upper plate was investigated in addition.

For the initial FE model the Serial DHO base is mounted only at several small cylindric elevations (see Figure 7 left). Here, the lower part of the base is free to move between the elevations and, due to the elasticity of the Serial DHO base, the motion of the oscillating mass will be disturbed. This, however, cannot be represented with the model according to Equation (5).

As a modification the Serial DHO base was therefore mounted at the complete lower base ring instead (see Figure 7 right). Figure 8 shows the corresponding FRF results. By increasing the contact region, the residual systematic error can effectively be reduced. Thus, for the real test bench, similar mounting conditions should be realized in order to obtain correct FRF results.

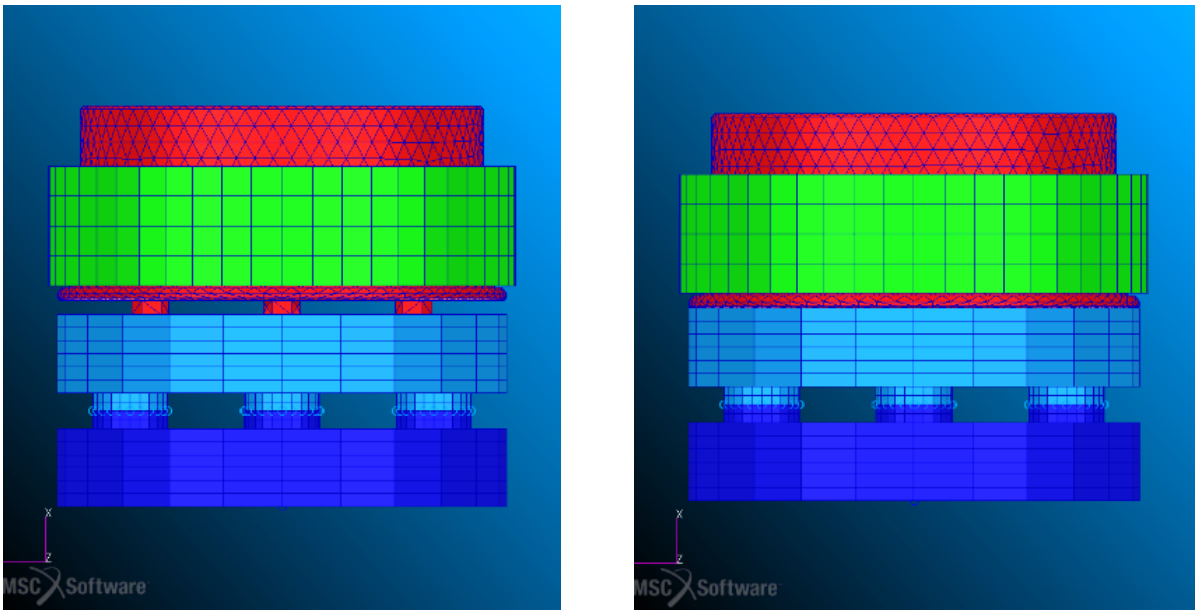

Figure 7: Mounting conditions – left on cylindric elevations only / right on complete base ring

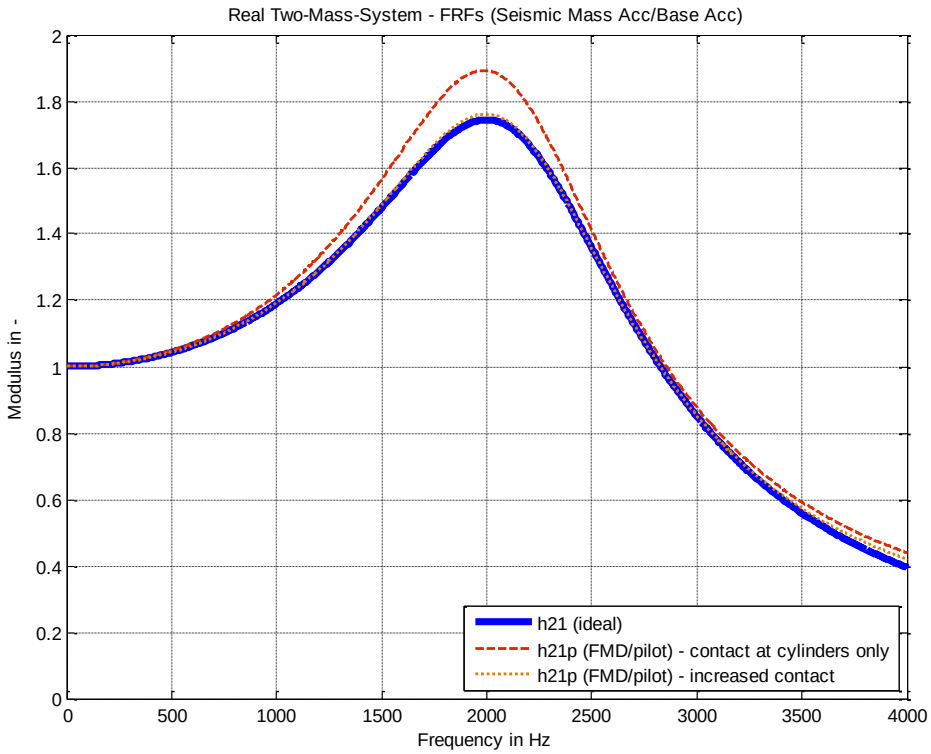

Bild 8: Ideal FRF (h21) vs. FRF (h21p) according to Equation (5) – initial/increased contact

2.2 Verification

2.2.1 Test setup and FMD calibration

The test setup is shown in Figure 9. On the left-hand side, no DHO payload is mounted on the FMD. The base mass m_1 in this case is about 1.3 kg. On the right-hand side, a DHO with Fumo base is mounted. In addition, three triaxial accelerometers are attached under 0°/120°/180° on the oscillating mass m_2. These sensors can be used to assess the quality of the identification result according to Equation (5) in comparison to the ideal results (i.e. the mean vertical acceleration of the oscillating mass from the additional sensors related to the base acceleration of the pilot sensor).

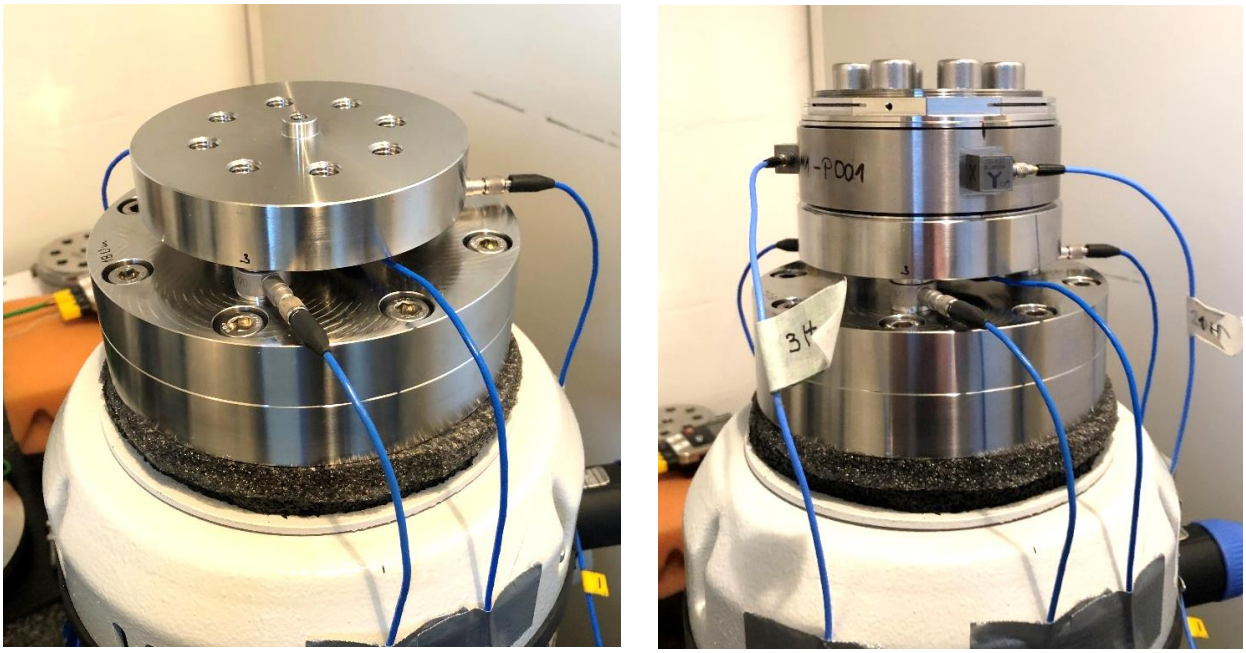

Figure 9: Test Setup with Fumo base – left w/o DHO payload / right with Fumo DHO

The calibration curves from the setup described above are shown in Figure 11. In the upper plot the force modulus (amplitude) of the three averaged forces normalized by the base acceleration, in the lower the corresponding phase is show. The ideal curves (red/solid in Figure 11) in this case equal to the base mass m_1 for the modulus and 0 rad for the phase.

The measured curves using nominal calibration values for all sensors (blue/dotted in Figure 11) show clearly visible deviations from the ideal curves. Thus, in order to properly calibrate the FMD calibration curves were derived for modulus and phase individually. For the modulus a quadratic fit, for the phase a linear fit was selected.

Applying the derived calibration curves to the measured data leads to corrected force curves (green/dash-dotted in Figure 11). It can be noticed that the calibration allows for a well representation of the ideal curves. Thus, in the following, the calibration will be applied in to all FMD measurements in order to derive the correct interface force.

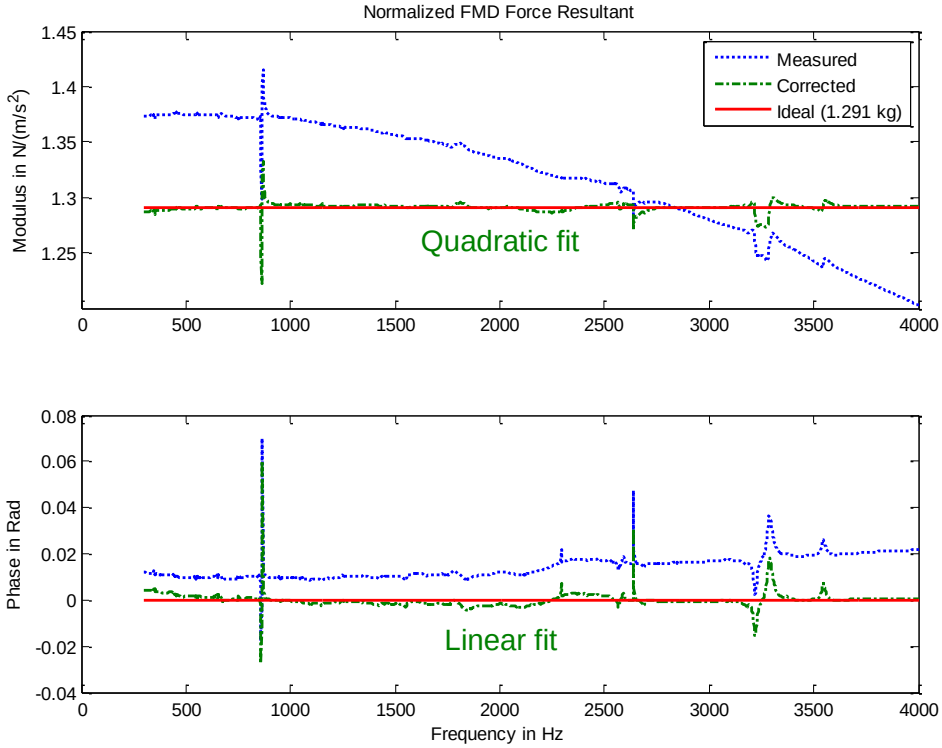

Figure 10: FMD calibration curves

2.2.2 DHO results

In a next step, the DHO with Fumo base according to Figure 9, right, was mounted on the FMD. The results are shown in Figure 11.

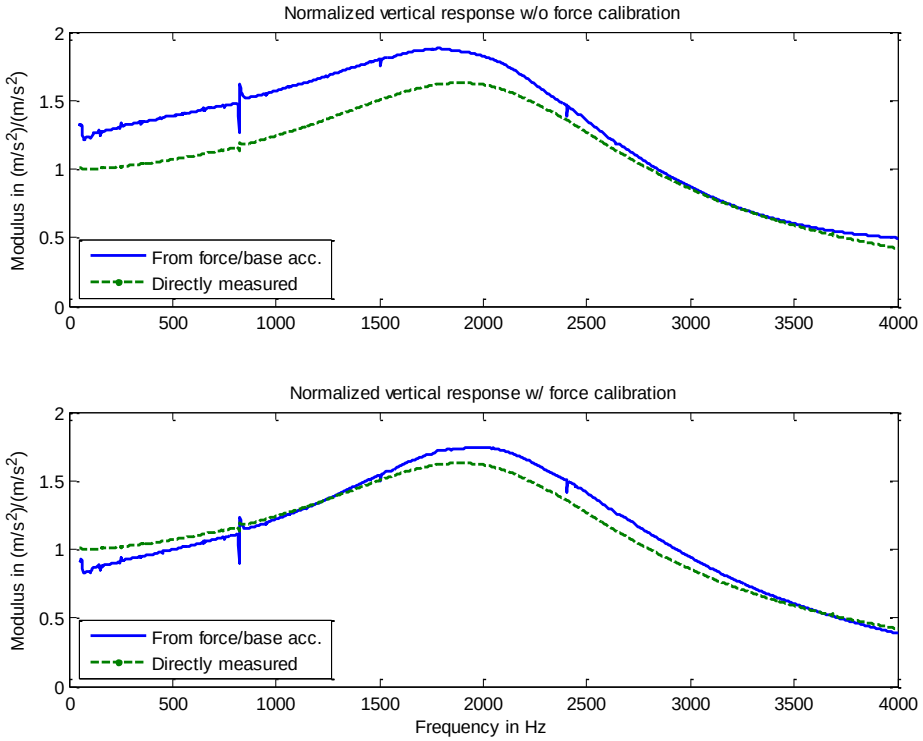

Figure 11: Results for Fumo DHO

In the upper plot of Figure 11 the results without FMD calibration are shown in order to assess the improvement with calibration when using the test bench with payload. It can be seen that the characteristics of the curves differ without calibration. Also, a significant shift of the peak frequency can be observed.

The corresponding curves with FMD calibration are presented in the lower plot of Figure 11. A clear improvement of the characteristics is observed. However, a – yet smaller – peak shift can still be observed which leaves room for improvement of the procedure.

2.3 Summary and conclusions

In this paper an approach to identify the DHO oscillating mass motion from base data was presented. In this context, a test bench with FMD was developed in order to measure the base acceleration and base force required by the method.

First measurements were very promising and indicate that the test bench can be used with minor improvements to obtain the desired data. Ongoing work is primarily directed to checking and improving the calibration. In particular, the calibration data of the individual acceleration sensors (pilot sensor and additional sensors on oscillating mass) are in focus in order to explain the residual mismatches between ideal response and the response obtained from the presented approach.